Chapter 4

Unimodal Sea States: Numerical Modelling

This Chapter outlines the parametric procedure for unimodal sea state conditions. The following sections provide a detailed description of the numerical procedure, using the same symbol and nomenclature adopted in Piscopo et al. (2024).

4.1 Main Assumptions

The sea state assessment procedure is based on the following assumptions:

I. Ship motions are linearly dependent on the amplitude of the incident waves;

II. Heave, pitch and roll accelerations are considered stationary processes over one-hour time intervals;

III. The speed-dependent ship transfer functions are preliminary known;

IV. The sea state conditions are assumed to be unimodal and short-crested.

The reference body frame has its origin at the ship center of mass, with x, y and z-axes forward, starboard and upward positive respectively, as depicted in Figure 6.1.

4.2 Measured ship acceleration spectra

Under the previous assumptions and notations, the Hermitian[4] cross-spectrum matrix of the measured ship accelerations in the encounter frequency domain $S_{ij}(\omega_e)$ is computed using the *cpsd* function available in MATLAB MathWorks (2024). The time series of the ship accelerations are denoted as a_k, where the subscript refers to the $k-th$ motions made out is equal to

[4]Hermitian matrix is a complex square matrix that is equal to its own conjugate transpose, i.e., $S_{ij}(\omega_e) = \overline{S_{ji}(\omega_e)}$

3, 4 and 5, for the heave pitch and roll motion, respectively. By combining two discrete-time signals a_i and a_j at the encounter frequency (ω_e), the cross spectral matrix $\hat{S}_{ij}(\omega_e)$ is given by Equation 4.1:

$$\hat{S}_{ij}(\omega_e) = \begin{bmatrix} \hat{S}_{33}(\bullet) & \hat{S}_{34}(\bullet) & \hat{S}_{35}(\bullet) \\ \hat{S}_{43}(\bullet) & \hat{S}_{44}(\bullet) & \hat{S}_{45}(\bullet) \\ \hat{S}_{53}(\bullet) & \hat{S}_{54}(\bullet) & \hat{S}_{55}(\bullet) \end{bmatrix} = \Re\{\hat{S}(\omega_e)\} + \Im\{\hat{S}(\omega_e)\}i \tag{4.1}$$

where the diagonal terms represent the real-valued power spectral densities of heave, roll and pitch accelerations, while the off-diagonal terms represent the corresponding complex-valued cross-power spectral densities. The Hermitian matrix in Equation 4.1 can be decomposed as the sum of a real symmetric and an imaginary antisymmetric parts. The real symmetric component, denoted by $\Re\{\hat{S}(\omega_e)\}$, has the diagonal elements corresponding to the power spectral densities of the measured signals, while the off-diagonal elements represent the cospectra. The imaginary part $\Im\{\hat{S}(\omega_e)\}$ is an antisymmetric matrix, with zero values along the diagonal, and off-diagonal elements corresponding to the quadrature spectra of each pair of signals. These matrices are defined by Equations 4.2 and 4.3, respectively.

$$\Re\{\hat{S}(\omega_e)\} = \begin{bmatrix} \hat{S}_{33}(\bullet) & \Re\{\hat{S}_{34}(\bullet)\} & \Re\{\hat{S}_{35}(\bullet)\} \\ \Re\{\hat{S}_{34}(\bullet)\} & \hat{S}_{44}(\bullet) & \Re\{\hat{S}_{45}(\bullet)\} \\ \Re\{\hat{S}_{35}(\bullet)\} & \Re\{\hat{S}_{45}(\bullet)\} & \hat{S}_{55}(\bullet) \end{bmatrix} \tag{4.2}$$

$$\Im\{\hat{S}(\omega_e)\} = \begin{bmatrix} 0 & \Im\{\hat{S}_{34}(\bullet)\} & \Im\{\hat{S}_{35}(\bullet)\} \\ -\Im\{\hat{S}_{34}(\bullet)\} & 0 & \Im\{\hat{S}_{45}(\bullet)\} \\ -\Im\{\hat{S}_{35}(\bullet)\} & -\Im\{\hat{S}_{45}(\bullet)\} & 0 \end{bmatrix} \tag{4.3}$$

By analysing the cross-spectral matrix decomposition, it can be noted that the ship accelerations can be evaluated considering:

I. Three power spectral densities derived from measured accelerations;

II. Three cospectra that represent the in-phase components of each pair of signals;

III. Three quadrature spectra represent the out-of-phase components of each pair of signals.

4.3 Tentative ship acceleration spectra

The parametric procedures assume that directional wave spectra are modelled using a set of parameterised theoretical spectra (e.g., JONSWAP or Bretschneider spectra). In this parametric procedure, the Joint North Sea Wave Project (JONSWAP) spectrum is adopted to identify the optimal tentative spectrum, which depends on the significant wave height, the wave peak period and the peak enhancement factor, as discussed in Chapter 2. Therefore, the tentative

cross-spectral matrix $\tilde{S}(\omega_e)$ can be determined by Equation 4.4:

$$\tilde{S}_{ij}\left(\tilde{T}_{p,\tilde{n}},\, \tilde{\gamma}_{\tilde{n}},\, \tilde{\mu}_{\tilde{n}},\, \omega_e\right) = \int_{-\frac{\pi}{2}}^{\frac{\pi}{2}} \tilde{s_{ij}}(\tilde{T}p,\, \tilde{\gamma},\, \tilde{\mu},\, \tilde{n}, \omega_e, \theta)\omega_e^4 d\theta \tag{4.4}$$

where $\tilde{s_{ij}}$ corresponds to the spectral function of the tentative ship accelerations for a unitary wave height, given by Equation 4.5:

$$\tilde{s}_{ij}\left(\tilde{T}_{p,\tilde{n}}, \tilde{\gamma}_{\tilde{n}}, \tilde{\mu}_{\tilde{n}}, \omega_e, \vartheta\right) = \begin{cases} H_i(\tilde{\mu}_{\tilde{n}} + \vartheta, \omega, \omega_e)\,\overline{H_j}(\tilde{\mu}_{\tilde{n}} + \vartheta, \omega, \omega_e)\,\tilde{S}_{e,1}(\bullet); \\ \quad \tilde{\mu}_{\tilde{n}} + \vartheta \in \left[\frac{\pi}{2}, \frac{3\pi}{2}\right] \\ \sum_{k=1}^{3} H_i(\tilde{\mu}_{\tilde{n}} + \vartheta, \omega_k, \omega_e)\,\overline{H_j}(\tilde{\mu}_{\tilde{n}} + \vartheta, \omega_k, \omega_e)\,\tilde{S}_{e,1}^{k}(\bullet); \\ \quad \tilde{\mu}_{\tilde{n}} + \vartheta \in \left[0, \frac{\pi}{2}\right[\cup \left]\frac{3\pi}{2}, 2\pi\right] \end{cases} \tag{4.5}$$

having denoted by $\tilde{S}_{e,1}$ the tentative wave spectrum in the encounter frequency domain with unitary significant wave height, by ω the absolute wave frequency corresponding to ω_e or ω_k if the relationship between the absolute and encounter frequency is bijective or the 3-to-1 multivalued problem occurs. In Equation 4.5 H_i is the complex transfer function of the $i-th$ motion mode, to be determined as a function of the ship main hydrodynamic properties as follows:

$$H(\tilde{\mu}_n + \vartheta, \omega, \omega_e) = \begin{bmatrix} H_3(\tilde{\mu}_n + \vartheta, \omega, \omega_e) \\ H_5(\tilde{\mu}_n + \vartheta, \omega, \omega_e) \\ H_4(\tilde{\mu}_n + \vartheta, \omega, \omega_e) \end{bmatrix} = \begin{bmatrix} \frac{q_{55}(\omega_e) f_3(\tilde{\mu}_n + \vartheta, \omega) - q_{35}(\omega_e) f_5(\tilde{\mu}_n + \vartheta, \omega)}{q_{33}(\omega_e) q_{55}(\omega_e) - q_{35}(\omega_e) q_{53}(\omega_e)} \\ \frac{q_{33}(\omega_e) f_5(\tilde{\mu}_n + \vartheta, \omega) - q_{53}(\omega_e) f_3(\tilde{\mu}_n + \vartheta, \omega)}{q_{33}(\omega_e) q_{55}(\omega_e) - q_{35}(\omega_e) q_{53}(\omega_e)} \\ \frac{f_4(\tilde{\mu}_n + \vartheta, \omega)}{q_{44}(\omega_e)} \end{bmatrix} \tag{4.6}$$

with:

$$q_{ij}(\omega_e) = -\omega_e^2(M_{ij} + A_{ij}) + i\omega_e B_{ij} + C_{ij} \tag{4.7}$$

where M_{ij} is the ship generalized mass for the i,j-th motion mode. The zero-speed added masses A_{ij} of heave, pitch and roll have been determined by the open-source code NEMOH and corrected to account for the forward speed effect, based on the formulation provided in Salvesen et al. (1970), according to Equation 4.8:

$$\mathbf{A}(\omega_e, U) = \begin{bmatrix} A_{33}(\omega_e, U) \\ A_{35}(\omega_e, U) \\ A_{53}(\omega_e, U) \\ A_{55}(\omega_e, U) \\ A_{44}(\omega_e, U) \end{bmatrix} = \begin{bmatrix} A^0_{33}(\omega_e) \\ A^0_{35}(\omega_e) - \frac{U}{\omega_e^2} B^0_{33}(\omega_e) \\ A^0_{53}(\omega_e) + \frac{U}{\omega_e^2} B^0_{33}(\omega_e) \\ A^0_{55}(\omega_e) + \frac{U^2}{\omega_e^2} A^0_{33}(\omega_e) \\ A^0_{44}(\omega_e) \end{bmatrix} \tag{4.8}$$

Similarly, the speed-dependent hydrodynamic dappings B_{ij} have also been corrected as follows:

$$\mathbf{B}(\omega_e, U) = \begin{bmatrix} B_{33}(\omega_e, U) \\ B_{35}(\omega_e, U) \\ B_{53}(\omega_e, U) \\ B_{55}(\omega_e, U) \\ B_{44}(\omega_e, U) \end{bmatrix} = \begin{bmatrix} B^0_{33}(\omega_e) \\ B^0_{35}(\omega_e) - \frac{U}{\omega_e^2} A^0_{33}(\omega_e) \\ B^0_{53}(\omega_e) + \frac{U}{\omega_e^2} A^0_{33}(\omega_e) \\ B^0_{55}(\omega_e) + \frac{U^2}{\omega_e^2} B^0_{33}(\omega_e) \\ B^0_{44}(\omega_e) \end{bmatrix} \tag{4.9}$$

Finally, the hydrostatic restoring coefficients, which are independent of frequency and forward ship of the ship, are computed according to Equation 4.10:

$$C_{ij} = \begin{bmatrix} C_{33} \\ C_{35} = C_{53} \\ C_{55} \\ C_{44} \end{bmatrix} = \begin{bmatrix} \rho g A_{WP} \\ -\rho g M_{WP} \\ \rho g I_{WP} \\ \rho g \nabla \overline{GM} \end{bmatrix} \tag{4.10}$$

where A_{WP} is the waterplane area, M_{WP} and I_{WP} are the first and second moments of the waterplane area with respect to the center of flotation, ∇ is the displaced volume of the ship and $\overline{GM}$ is the metacentric height.

4.4 Spearman rank correlation

Once the measured and tentative wave spectra are computed at each encounter wave frequency, the Spearman correlation coefficient $\tilde{c}_{ij}$ between measured $\hat{S}_{ij}(\bullet)$ and tentative $\tilde{S}_{ij}$ ship acceleration spectra is computed according to Equation 4.11:

$$\tilde{c}_{ij}(\tilde{T}_{p,\tilde{n}}, \tilde{\gamma}_{\tilde{n}}, \tilde{\mu}_{\tilde{n}}) = \frac{\operatorname{cov}\left\{R(\hat{S}_{ii}(\bullet)), R(\tilde{S}_{ij}(\bullet))\right\}}{\operatorname{std}\left\{R(\hat{S}_{ii}(\bullet))\right\} \bullet \operatorname{std}\left\{R(\tilde{S}_{ij}(\bullet))\right\}} \tag{4.11}$$

where R is the rank of the variable associated to the measured $\hat{S}_{ii}(\bullet)$ and the tentative wave spectra $\tilde{S}_{ij}(\bullet)$. Hence, nine correlation coefficients can be separately determined, based on the power spectral densities of measured accelerations, as well as the cospectra and quadrature spectra of each couple of signals. The correlation coefficient computed for the real $\tilde{c}^{r}{}_{ij}$ and imaginary $\tilde{c}^{i}{}_{ij}$ parts of the cross-spectra are provided by Equations 4.12 and 4.13, respectively:

$$\tilde{c}^{r}_{ij}(\tilde{T}_{p,\tilde{n}}, \tilde{\gamma}_{\tilde{n}}, \tilde{\mu}_{\tilde{n}}) = \frac{\mathrm{cov}\left\{R\left(\left|\Re\left\{\hat{S}_{ij}(\bullet)\right\}\right|\right), R\left(\left|\Re\left\{\hat{S}_{ii}(\bullet)\right\}\right|\right)\right\}}{\mathrm{std}\left\{R\left(\left|\Re\left\{\hat{S}_{ij}(\bullet)\right\}\right|\right)\right\} \bullet \mathrm{std}\left\{R\left(\left|\Re\left\{\hat{S}_{ii}(\bullet)\right\}\right|\right)\right\}} \tag{4.12}$$

$$\tilde{c}^{i}_{ij}(\tilde{T}_{p,\tilde{n}}, \tilde{\gamma}_{\tilde{n}}, \tilde{\mu}_{\tilde{n}}) = \frac{\mathrm{cov}\left\{R\left(\left|\Im\left\{\hat{S}_{ij}(\bullet)\right\}\right|\right), R\left(\left|\Im\left\{\hat{S}_{ii}(\bullet)\right\}\right|\right)\right\}}{\mathrm{std}\left\{R\left(\left|\Im\left\{\hat{S}_{ij}(\bullet)\right\}\right|\right)\right\} \bullet \mathrm{std}\left\{R\left(\left|\Im\left\{\hat{S}_{ii}(\bullet)\right\}\right|\right)\right\}} \tag{4.13}$$

To determine the mean correlation coefficient between the measured and tentative cross-spectral matrices and reduce its variance, each correlation coefficient shall be preliminarily subjected to the Fisher z-transformation (Fisher, 1921), according to Equation 4.14:

$$\tilde{c}_{\tilde{s}}(\tilde{T}_{p,\tilde{n}}, \tilde{\gamma}_{\tilde{n}}, \tilde{\mu}_{\tilde{n}}) = \tanh^{-1}\left[\frac{\sum_i \tanh \tilde{c}_{ij}(\bullet)}{3}\right] \forall i = 3,4,5 \tag{4.14}$$

having denoted by $\tilde{c}_{\tilde{s}}$ the tentative Spearman correlation coefficient.

4.5 Assessment of the main wave parameters

As the last step of the numerical procedure the main wave parameters can be estimated, keeping in mind that the heading angle of the prevailing wave direction is measured relative to the ship bow as shown in Figure 4.1 and the compass angle of each wave train relative to the ship reference frame is defined by β, as depicted in Figure 4.2.

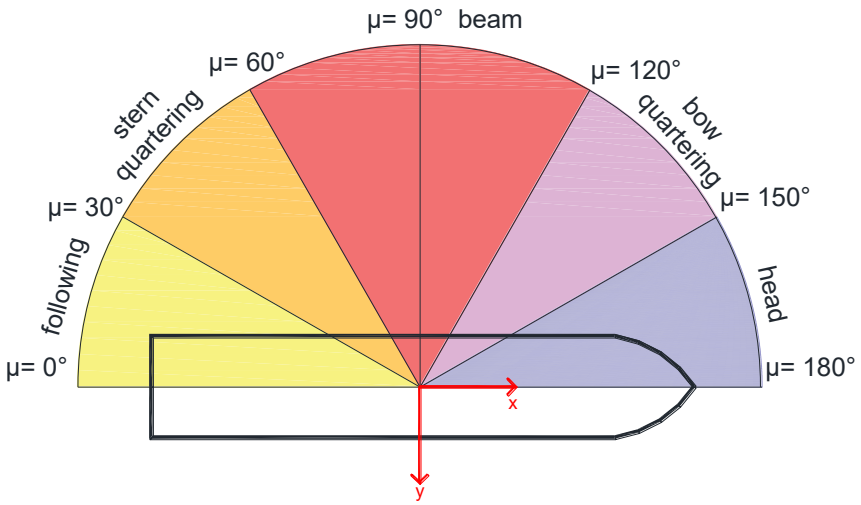

Figure 4.1: Heading angles

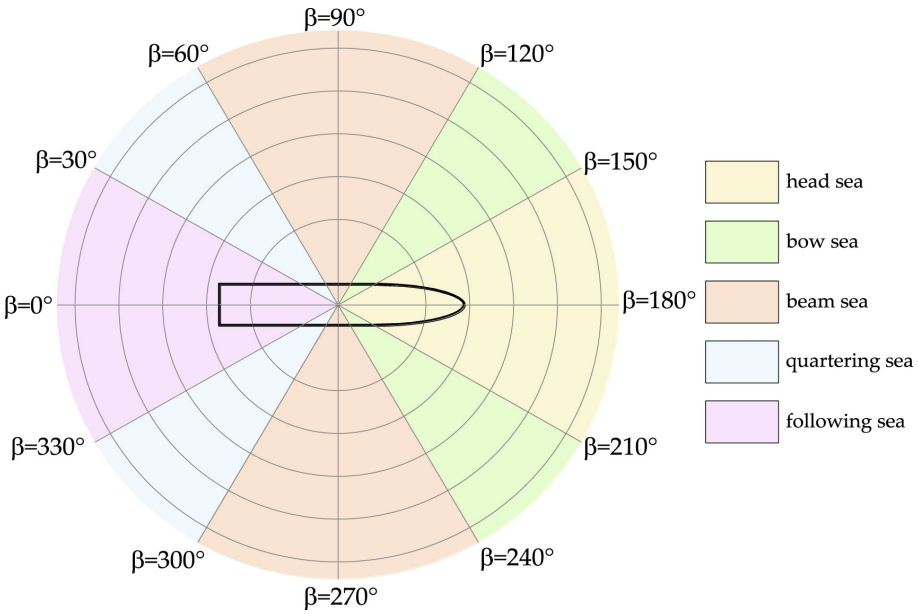

Figure 4.2: Compass angles.

By iteratively varying the wave peak period, the peak enhancement factor and the heading angle of prevailing wave direction, the sea spectra parameters that maximise the Spearman rank correlation coefficient and represent the most probable sea state parameters encountered by the ship along its route can be determined by Equation 4.15:

$$\left\{\overline{T}_{p,\tilde{n}}, \overline{\gamma}_{\tilde{n}}, \overline{\mu}_{\tilde{n}}\right\} : \tilde{c}_{\tilde{s}}(\overline{T}_{p,\tilde{n}}, \overline{\gamma}_{\tilde{n}}, \overline{\mu}_{\tilde{n}}) = \max\left\{\tilde{c}_{\tilde{s}}(\tilde{T}_{p,\tilde{n}}, \tilde{\gamma}_{\tilde{n}}, \tilde{\mu}_{\tilde{n}})\right\}$$
$$\forall\left\{\tilde{T}_{p,\tilde{n}}, \tilde{\gamma}_{\tilde{n}}, \tilde{\mu}_{\tilde{n}}\right\} \in [T_{p,\min}, T_{p,\max}] \times [1, \gamma_{\max}] \times [0, \pi] \quad (4.15)$$

Subsequently, the significant wave height H_s is estimated as the ratio of measured to tentative ship acceleration spectra for unit wave amplitude and the i-th motion mode according to Equation 4.16:

$$\overline{H}^{ii}_{s,\tilde{n}}\,(\overline{T}_{p,\tilde{n}}, \overline{\gamma}_{\tilde{n}}, \overline{\mu}_{\tilde{n}}) = \sqrt{\frac{\int \hat{S}_{ii}(\omega_e)d\omega_e}{\int \tilde{S}_{ii}(\overline{T}_{p,\tilde{n}}, \overline{\gamma}_{\tilde{n}}, \overline{\mu}_{\tilde{n}})d\omega_e}} \forall i = 3, 4, 5, \quad (4.16)$$

To reduce the variance in the assessment of singular wave height , H_s is finally estimated by Equation 4.17:

$$\overline{H}_{s,\tilde{n}}\,(\overline{T}_{p,\tilde{n}}, \overline{\gamma}_{\tilde{n}}, \overline{\mu}_{\tilde{n}}) = \frac{1}{3}\sum_{i=3}^{5} \overline{H}^{ii}_{s}\,(\overline{T}_{p,\tilde{n}}, \overline{\gamma}_{\tilde{n}}, \overline{\mu}_{\tilde{n}}) \quad (4.17)$$

Equations 4.16 and 4.17 are iteratively repeated by varying the spreading number from 2 to 4 until the value that minimises the standard deviation of H_s is detected according to Equation

4.18:

$$\overline{n} : std\left\{\overline{H}_{s,\tilde{n}}^{ii}\left(\overline{T}_{p,\tilde{n}}, \overline{\gamma}_{\tilde{n}}, \overline{\mu}_{\tilde{n}}\right)\right\} = min\left\{std\left\{\overline{H}_{s,\tilde{n}}^{ii}\left(\overline{T}_{p,\tilde{n}}, \overline{\gamma}_{\tilde{n}}, \overline{\mu}_{\tilde{n}}\right)\right\}\right\}$$
$$\forall \tilde{n} \in [n_{min}, n_{max}] \forall i = 3,4,5 \quad (4.18)$$

The last step of this procedure is devoted to estimating the direction of the heading angle of the prevailing wave direction on the iterative computation limited to the interval of $[0, \pi]$ to reduce the computational effort but it can be easily extended to the interval $[0, 2\pi]$ by Equation 4.19 based on the sign of the correlation coefficient of the quadrature spectrum involving the antisymmetric roll motion according to Equation 4.19:

$$\overline{\beta}\overline{n} = \begin{cases} \overline{\mu}_{\overline{n}}, & \text{if } \dfrac{\operatorname{cov}\left\{R\left(\left|\Im\left\{\hat{S}_{34}(\bullet)\right\}\right|\right), R\left(\left|\Im\left\{\overline{S}_{34}(\bullet)\right\}\right|\right)\right\}}{\operatorname{std}\left\{R\left(\left|\Im\left\{\hat{S}_{34}(\bullet)\right\}\right|\right)\right\} \bullet \operatorname{std}\left\{R\left(\left|\Im\left\{\overline{S}_{34}(\bullet)\right\}\right|\right)\right\}}, \\ 2\pi - \overline{\mu}_{\overline{n}}, & \text{if } \dfrac{\operatorname{cov}\left\{R\left(\left|\Im\left\{\hat{S}_{34}(\bullet)\right\}\right|\right), R\left(\left|\Im\left\{\overline{S}_{34}(\bullet)\right\}\right|\right)\right\}}{\operatorname{std}\left\{R\left(\left|\Im\left\{\hat{S}_{34}(\bullet)\right\}\right|\right)\right\} \bullet \operatorname{std}\left\{R\left(\left|\Im\left\{\overline{S}_{34}(\bullet)\right\}\right|\right)\right\}}. \end{cases} \quad (4.19)$$

4.6 Extended Unimodal procedure

The numerical procedure outlined in the previous Sections 4.1-4.5 has been extended and included in the algorithm for estimating the bimodal short-crested sea state conditions, as presented in Chapter 5.

In particular, the computation of the 3×3 Hermitian matrix of heave, roll and pitch accelerations remains unchanged (as detailed in Section 4.2).

The cross-power spectral matrix is computed for any tentative values of $\tilde{T}_p$ and $\tilde{\gamma}$, according to Equation 4.20:

$$\tilde{S}_{ij}(\tilde{T}_p, \tilde{\gamma}, \omega_e) = \int_{-\pi/2}^{\pi/2} \tilde{h}_{ij}(\tilde{T}_p, \tilde{\gamma}, \omega_e)\, \omega_e^4\, d\theta \quad (4.20)$$

where $\tilde{h}_{ij}$ in Equation 4.20 denotes the ship acceleration transfer function, defined in Equation 4.21:

$$\tilde{h}_{ij}(\tilde{T}_p, \tilde{\gamma}, \omega_e) = \begin{cases} H_i(\beta + \vartheta, \omega_e)\, H_j^*(\beta + \vartheta, \omega_e)\, \tilde{S}_e(\tilde{T}_p, \tilde{\gamma}, \omega_e), \\ \quad \text{if} \psi \leq 0 \ \text{ or } \psi > 0 \wedge \omega_e \geq \frac{1}{4}\psi, \\ \sum_{k=1}^{3} H_i^k(\beta + \vartheta, \omega_e)\, H_j^{k*}(\beta + \vartheta, \omega_e)\, \tilde{S}_e^k(\tilde{T}_p, \tilde{\gamma}, \omega_e), \\ \quad \text{otherwise.} \end{cases} \quad (4.21)$$

where H_i is the ship complex transfer function and the asterisk denotes the relevant complex conjugate value.

Subsequently, the mean Pearson correlation coefficient of the tentative ship acceleration spectra (Gibbons, 1985) as regards the measured ones can be determined by Equation 4.22, based

on the z-transformation (Fisher, 1921):

$$\tilde{c}(\tilde{T}_p, \tilde{\gamma}) = \tanh^{-1}\frac{1}{9}\left[\sum_{i=3}^{5}\tanh\tilde{c}_{ii} + \sum_{i=3}^{5}\sum_{j>i}^{5}\left(\tanh\tilde{c}_{ij}^{r} + \tanh\tilde{c}_{ij}^{i}\right)\right] \tag{4.22}$$

where: $\tilde{c}_{ii}$ is the correlation coefficient of heave 3, roll 4 and pitch 5 tentative acceleration spectra and $c_{ij}^{r}(c_{ij}^{i})$ is the correlation coefficient of the real (imaginary) part of the cross-power spectral density of combined i,j-th motions.

Finally, the sea state parameters are estimated by Equation 4.23 that is based on finding the maximum of the Pearson correlation coefficient:

$$\{\bar{T}_p, \bar{\gamma}\} : \tilde{c}(\bar{T}_p, \bar{\gamma}) = max\{\tilde{c}(\tilde{T}_p, \tilde{\gamma})\}\forall\{\tilde{T}_p, \tilde{\gamma}\} \tag{4.23}$$

The significant wave height is then determined by Equation 4.24, where the heave acceleration spectrum is employed, provided that it is the most significant one:

$$\bar{H}_s = \sqrt{\frac{\int_0^\infty S_{33}(\omega_e)d\omega_e}{\int_0^\infty \bar{S}_{33}(\bar{T}_p, \bar{\gamma}, \omega_e)d\omega_e}} \tag{4.24}$$

The main differences highlighted in this extended version of the unimodal short-crested procedure are as follows: (i) the computation of the tentative wave spectra is independent of the tentative heading angle values; (ii) the Pearson linear correlation coefficient is employed to define the correlation between the measured and tentative wave spectra; (iii) nine correlation coefficients are included in Equation 4.22; (iv) only the heave acceleration spectrum is used to determine the significant wave height and (v) the spreading number is fixed.

Chapter 5

Bimodal Sea State: Numerical Modelling

This Chapter presents the extension of the parametric motel to obtained by the superposition of wind and swell components. The numerical model adopts the same notation as in Piscopo et al. (2025).

5.1 Preliminary remarks

The bimodal wave spectra are generally based on the linear superposition of wind sea and swell (DNV, 2017), according to Equation 5.1:

$$S_b(\omega, \theta) = S(\omega, H_{s,w}, T_{p,w}, \gamma_w)D(\theta, n_w) + S(\omega, H_{s,s}, T_{p,s}, \gamma_s)D(\theta, n_s) \tag{5.1}$$

where: S is the JONSWAP spectrum, ω is the absolute wave frequency, $H_{s,w}(H_{s,s})$ is the wind sea (swell) significant wave height, $T_{p,w}(T_{p,s})$ is the wind sea (swell) wave peak period, $\gamma_w(\gamma_s)$ is the wind sea (swell) peak enhancement factor, n_w (n_s) is the wind sea (swell) spreading factor, θ is the single wave train angle, measured from the prevailing wave direction and D is the directional spreading function (DNV, 2017) computed according to Equation 3.2.
The numerical procedure employs the wind sea and swell prevailing directions provided by an external weather forecast source, such as the ECMWF data (Kong et al., 2024) in order to reduce the computational effort and the possible uncertainness in the assessment of the above-mentioned parameters due to the Doppler shift effect. These datasets are employed in conjunction with the wave buoy analogy method to improve the reliability of the sea state estimation algorithm. Accordingly, as shown in the flowchart depicted in Figure 5.1, the wave forecast data are used to:

- preliminarily detect whether the sea state is unimodal or bimodal;
- provide the estimated wind sea and/or swell prevailing directions as input data for the sea state reconstruction algorithm.

In case of wind sea or swell-dominated sea state conditions, the relevant sea state parameters are estimated according to the procedure outlined in Section 4.6. Otherwise, wind sea and swell parameters are separately addressed, as outlined in Section 5.2, which deals with the extension of the algorithm to bimodal sea state conditions.

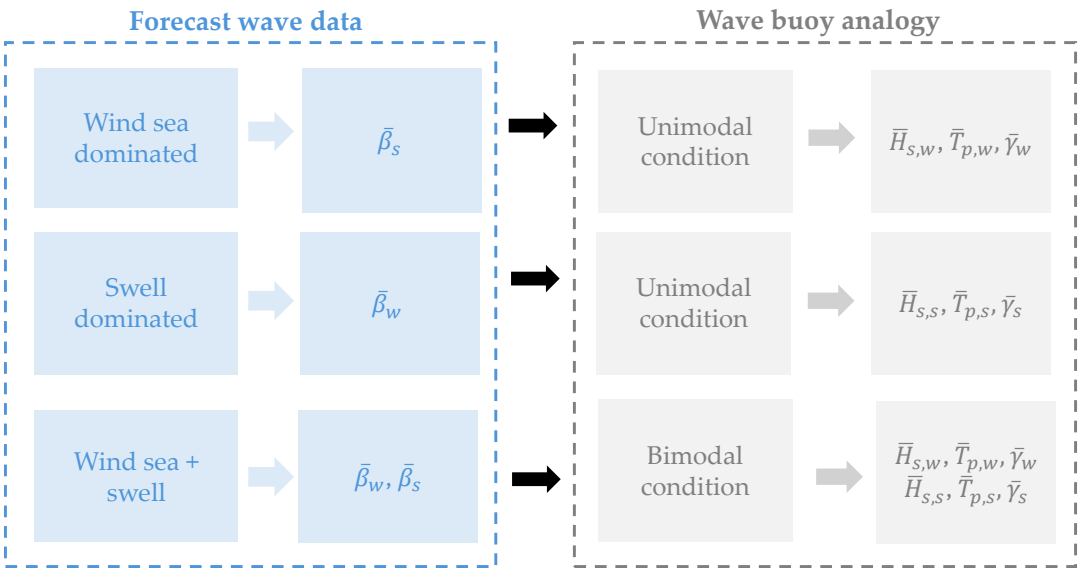

Figure 5.1: Flowchart of the sea state reconstruction algorithm

5.2 Numerical bimodal model

The procedure outlined in Section 4.6 can be extended to bimodal sea states by introducing the concept of tentative separation frequency $\tilde{\omega}_s$, in order to separately estimate the tentative wind sea acceleration time history $\tilde{a}_{i,w}$ by applying a high-pass filter to the initial signal, according to Equation 5.2:

$$\tilde{a}_{i,w}(t, \omega_s) = \text{highpass}(a_i(t) \,|\, \tilde{\omega}_s, \quad \forall i \in \{3, 4, 5\} \tag{5.2}$$

The tentative swell acceleration time history is determined by Equations 5.3, according to the linear superposition principle:

$$\tilde{a}_{i,s} = a_i(t) - \tilde{a}_{i,w}(t, \omega_s), \quad \forall i \in \{3, 4, 5\} \tag{5.3}$$

After determining the tentative high filtered signals, it is possible to evaluate the relevant 3×3 Hermitian matrices $\tilde{S}w(\omega_e)|\tilde{\omega}s$ and $\tilde{S}s(\omega_e)|\tilde{\omega}s$, conditioned on the tentative separation frequency $\tilde{\omega}s$ and separately apply the procedure outlined in Section 4.6.
Subsequently, the mean correlation coefficients $\bar{c}_w(\bar{T}_{p,w}, \bar{\gamma}_w)|\tilde{\omega}_s$ and $\bar{c}_s(\bar{T}_{p,s}, \bar{\gamma}_s)|\tilde{\omega}_s$, fulfilling Equation 4.22 and conditioned on $\tilde{\omega}s$ can be determined.

After estimating the wind sea and swell parameters for each tentative value of the separation frequency, the sea state parameters can be finally selected, as they correspond to the value $\bar{\omega}_s$ fulfilling the maximum condition provided by Equation 5.4:

$$\bar{\omega}_s : \bar{c}_w(\bar{T}_{p,w}, \bar{\gamma}_w)|\bar{\omega}_s + \bar{c}_s(\bar{T}_{p,s}, \bar{\gamma}_s)|\bar{\omega}_s = max\{\bar{c}_w(\bar{T}_{p,w}, \bar{\gamma}_w)|\bar{\omega}_s + \bar{c}_s(\bar{T}_{p,s}, \bar{\gamma}_s)|\bar{\omega}_s\} \quad \forall \tilde{\omega}_s \in [\tilde{\omega}_{s,min}, \tilde{\omega}_{s,max}] \tag{5.4}$$

where $\tilde{\omega}_{s,min}$, ($\tilde{\omega}_{s,max}$) is the lower (upper) bound of the tentative separation frequency interval corresponding to 2%(98%) of the power spectral density area of measured ship accelerations in the encounter wave frequency domain.
Hence, the equivalent significant wave height $\bar{H}_{s,eq}$ is determined by Equation 5.5:

$$\bar{H}_{s,eq} = \sqrt{\bar{H}_{s,w}^2 + \bar{H}_{s,s}^2} \tag{5.5}$$

while the prevailing direction of the equivalent sea state $\bar{\beta}_{eq}$ is determined by Equation 5.6:

$$\bar{\beta}_{eq} = \begin{cases} \bar{\beta}_{eq}^* & \text{if } 0 \le \bar{\beta}_{eq}^* \le 360° \\ \bar{\beta}_{eq}^* - 360° & \text{if } \bar{\beta}_{eq}^* > 360° \\ 360° + \bar{\beta}_{eq}^* & \text{if } \bar{\beta}_{eq}^* < 0° \end{cases} \tag{5.6}$$

$$\begin{cases} \bar{\beta}_w \frac{\bar{H}_{s,w}^2}{\bar{H}_{s,eq}^2} + \bar{\beta}_s \frac{\bar{H}_{s,s}^2}{\bar{H}_{s,eq}^2} & \text{if } |\bar{\beta}_s - \bar{\beta}_w| \le 180° \\ \bar{\beta}_w \frac{\bar{H}_{s,w}^2}{\bar{H}_{s,eq}^2} + \bar{\beta}_s \frac{\bar{H}_{s,s}^2}{\bar{H}_{s,eq}^2} - 360 \frac{(\bar{\beta}_s - \bar{\beta}_w)}{|\bar{\beta}_s - \bar{\beta}_w|} \frac{\bar{H}_{s,s}^2}{\bar{H}_{s,eq}^2} & \text{if } |\bar{\beta}_s - \bar{\beta}_w| > 180° \end{cases}$$

Finally, the wave energy period of the equivalent sea state $\bar{T}_{e,eq}$ is determined according to Equation 5.7:

$$\bar{T}_{e,eq} = \bar{T}_{e,w} \frac{\bar{H}_{s,w}^2}{\bar{H}_{s,eq}^2} + \bar{T}_{e,s} \frac{\bar{H}_{s,s}^2}{\bar{H}_{s,eq}^2} \tag{5.7}$$

where $\bar{T}_{e,w}(\bar{T}_{e,s})$ is the wind sea (swell) mean energy period to be determined by Equation 5.8:

$$\bar{T}_{e,w} = (0.7303 + 0.04936\bar{\gamma}_w - 0.006556\bar{\gamma}_w^2 + 0.000361\bar{\gamma}_w^3)\bar{T}_{p,w} \tag{5.8}$$

having denoted by $T_{p,w}$ and γ_w the wave peak period and peak enhancement factor (DNV, 2017). A similar expression holds for the swell wave component of the wind sea spectrum.

5.3 Range of application

In order to detect the range of application of the numerical procedure outlined in Section 5.2 a preliminary analysis is carried out. The time series are generated, using the code detailed in Chapter 3, by randomly varying the main sea state parameters as shown in Table 5.1.

The range of variation of the wind sea significant wave height and wave peak period covers about the 85% and 96% of relevant sea state conditions for world-wide trade (DNV, 2017). The range of variation of the swell parameters, instead, has been selected in order to cover the typical design conditions provided by the Offshore Standard "Position mooring" (DNV, 2010) off the coastlines of Nigeria, Gabon, Ivory Coast, Mauritania and Angola, where significant swell systems occur. Nevertheless, the algorithm has no limitations relative to the range of variation of the significant wave height and wave period.

Parameter	**Symbol**	**Wind sea**	**Swell**	**Unit**	**Value**
Significant wave height	$\{H_{s,w} \mid H_{s,s}\}$	0.5–5.0	0.5–5.0	[m]	random
Wave peak period	$\{T_{p,w} \mid T_{p,s}\}$	6–14	16–20	[s]	random
Shape parameter	$\{\gamma_w \mid \gamma_s\}$	1	8	[adim]	fixed
Spreading parameter	$\{n_w \mid n_s\}$	4	8	[adim]	fixed
Heading angle	$\{\beta_w \mid \beta_s\}$	0–180	-	[deg]	30 deg step
Ship speed	U	20	-	[kn]	fixed

Table 5.1: Main sea state parameters – preliminary analysis.

Hence, 20 ship motion time histories are simulated for each combination of wind sea and swell prevailing directions, by varying the heading angles in the range 0-180 deg with 30 deg step. Figure 5.2 depict the simulated β_{eq} versus the estimated $\bar{\beta}_{eq}$ equivalent heading angles on the x and $y-$ axes, respectively. More precisely, Figure 5.2 (a) refers each combination of wind sea and swell prevailing directions that rely on a high reliability of the algorithm, as proved by the Mean Absolute Error (MAE) that is equal to 5.068 deg. On the contrary, Figure 5.2 (b) provides the remaining combination of prevailing directions, corresponding to a low reliability of the algorithm, with a Mean Absolute Error (MAE) on the equivalent prevailing wave direction equal to 45.181 deg.

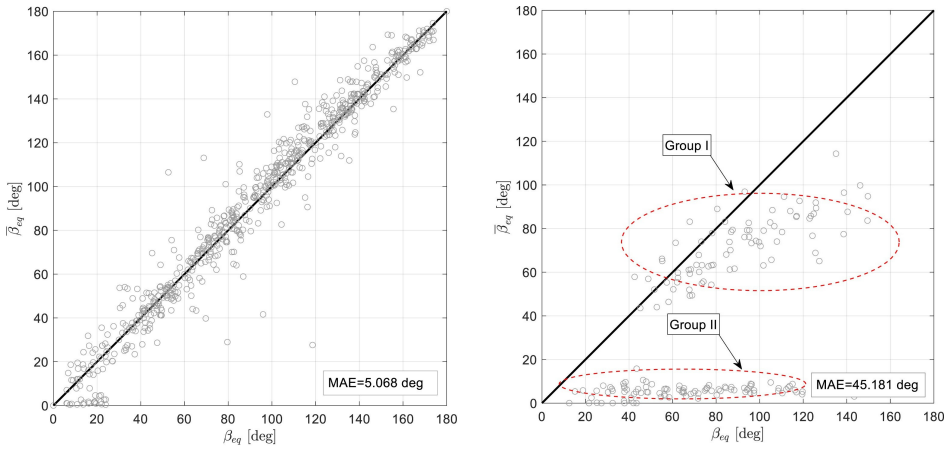

(a) Sea state conditions with high reliability of the algorithm

(b) Sea state conditions with low reliability of the algorithm

Figure 5.2: Equivalent heading angles.

This dataset can be further subdivided into two groups, namely the Group I that refers to sea state conditions with $\beta_w = 30°$ and $\beta_s \geq 90°$ and the Group II that refers to sea state conditions with $\beta_w = 0°$ and $\beta_s \geq 60°$. These outcomes highlight that the reliability of the algorithm is mainly affected by the Doppler shift and suggest to reduce its range of application as depicted in Figure 5.3, where the wind sea and swell prevailing direction domain is subdivided into two distinct areas. Area I (II) refers to all wind sea and swell prevailing directions that are expected to rely on a high (low) accuracy level of the sea state reconstruction algorithm.

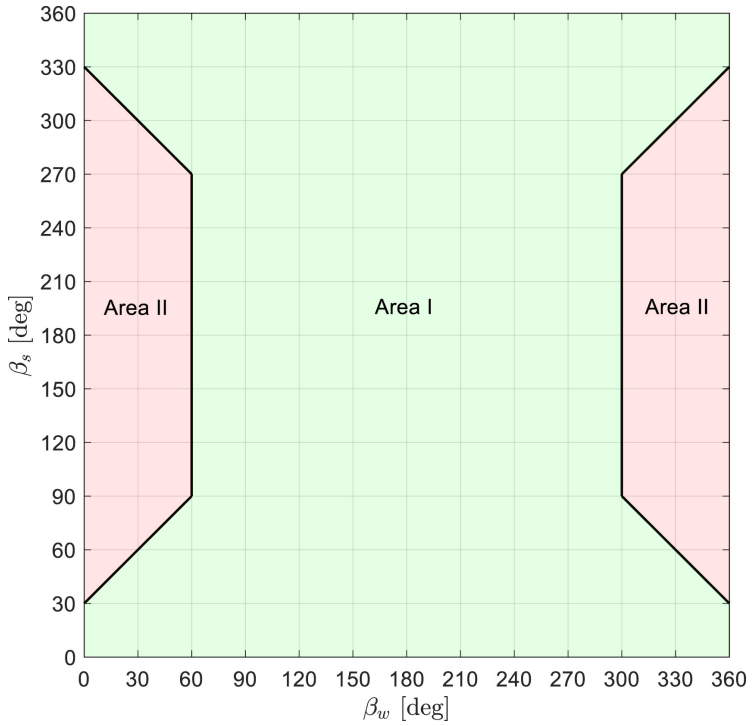

Figure 5.3: Range of application of the algorithm.

By Figure 5.3 it is gathered that the algorithm can be employed in almost the 83% of bimodal sea state conditions, even if this value is probably higher in real situations, as quartering and following seas lying in Area II are not common during navigation, to avoid possible ship dynamic instabilities, such as surf-riding and parametric roll (IMO, 2019). Hence, according to the findings of this preliminary investigation, the benchmark study will be carried out considering the wind sea and swell prevailing directions lying in Area I of Figure 5.3 (See Chapter 7).